

On the adiabatic preparation of spatially-ordered Rydberg excitations of atoms in a one-dimensional optical lattice by laser frequency sweeps

David Petrosyan

Institute of Electronic Structure and Laser, FORTH, GR-71110 Heraklion, Crete, Greece

Klaus Mølmer

Department of Physics and Astronomy, Aarhus University, DK-8000 Aarhus C, Denmark

Michael Fleischhauer

*Fachbereich Physik und Forschungszentrum OPTIMAS,
Technische Universität Kaiserslautern, D-67663 Kaiserslautern, Germany*

(Dated: March 25, 2018)

We examine the adiabatic preparation of crystalline phases of Rydberg excitations in a one-dimensional lattice gas by frequency sweep of the excitation laser, as proposed by Pohl *et al.* [Phys. Rev. Lett. **104**, 043002 (2010)] and recently realized experimentally by Schauß *et al.* [Science **347**, 1455 (2015)]. We find that the preparation of crystals of a few Rydberg excitations in a unitary system of several tens of atoms requires exceedingly long times for the adiabatic following of the ground state of the system Hamiltonian. Using quantum stochastic (Monte-Carlo) wavefunction simulations, we show that realistic decay and dephasing processes affecting the atoms during the preparation lead to a final state of the system that has only a small overlap with the target crystalline state. Yet, the final number and highly sub-Poissonian statistics of Rydberg excitations and their spatial order are little affected by the relaxations.

I. INTRODUCTION

Atoms in high-lying Rydberg states strongly interact with each other via the long-range dipole-dipole or van der Waals potentials [1, 2]. These interactions can suppress multiple Rydberg excitations of atoms within a certain blockade distance from each other [3], and are being explored for obtaining ordered phases of interacting many-body systems and simulating quantum phase transitions [4–13].

Several conceptually different approaches have been suggested for the preparation of crystalline order of Rydberg excitations in spatially-extended ensembles of cold atoms. These include direct (near-)resonant laser excitation of strongly-interacting Rydberg states in continuous or lattice gases [14–19], and the deceleration and storage in one-dimensional (1D) atomic medium of propagating light pulses forming the so-called Rydberg polaritons under the conditions of electromagnetically induced transparency [20, 21]. A common feature of all these schemes is that the resulting spatially-periodic structure of Rydberg excitations has finite density-density correlation length, while their number exhibits highly sub-Poissonian statistics characterized by negative Mandel parameter $Q \lesssim -0.5$. The Rydberg excitations then essentially form a liquid rather than a crystal phase with long-range order.

To achieve perfect Rydberg crystals with long – ideally infinite – correlation length, an adiabatic preparation protocol of the ground state of an Ising-type Hamiltonian for interacting Rydberg gases has been proposed [22–25]. An experimental realization involving a few Rydberg excitations in a 1D lattice of several tens of sites was recently reported in Ref. [26]. Our aim here is to critically

re-examine this protocol, taking into account realistic relaxation processes affecting the atoms. We find that, under typical experimental conditions, it is not feasible to attain the perfectly-ordered ground state of the Hamiltonian even for three or four Rydberg excitations in a finite 1D lattice gas. This is because the atomic decay and dephasing during the exceedingly long preparation time required for the adiabatic evolution of the system spoil the adiabaticity and significantly reduce the overlap of the final state of the system with the target ground state of the Hamiltonian. This overlap, or fidelity, is largest at some intermediate value of the preparation time, and maximizing the probability of the ordered state of Rydberg excitations requires therefore a compromise between the adiabatic following and decoherence. Even though the perfectly-ordered state cannot be obtained with high fidelity, good spatial ordering of Rydberg excitations is still achieved.

II. THE ADIABATIC PREPARATION PROTOCOL

We consider a system of N atoms trapped in a 1D optical lattice potential, with one atom per lattice site, assuming no site-occupation defects. A spatially-uniform time-dependent laser field couples the ground state $|g\rangle$ of each atom to the Rydberg state $|r\rangle$ with the Rabi frequency $\Omega(t)$ and detuning $\delta(t) \equiv \omega - \omega_{rg}$. In the frame rotating with the laser field frequency ω , the system is

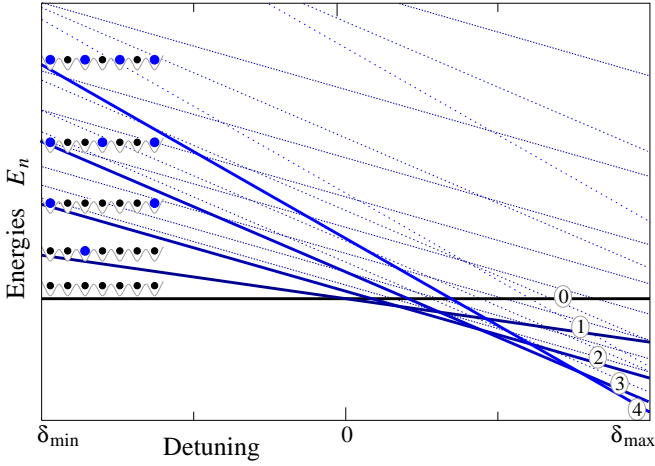


FIG. 1. Diagram of energies E_n of Hamiltonian (1) in the limit of $\Omega \rightarrow 0$ versus laser detuning δ , for $n = 0, 1, 2, 3, 4$ Rydberg excitations of atoms in a lattice. Thick lines correspond to the lowest energy E_n^{\min} within the n -excitation subspace, while thin dotted lines with the same slope (and color) denote the excited state energies with the same $n \geq 2$.

described by the Ising–spin- $\frac{1}{2}$ -like Hamiltonian

$$\mathcal{H}/\hbar = -\delta(t) \sum_j \hat{\sigma}_{rr}^j + \sum_{i < j} \Delta_{ij} \hat{\sigma}_{rr}^i \hat{\sigma}_{rr}^j - \Omega(t) \sum_j (\hat{\sigma}_{rg}^j + \hat{\sigma}_{gr}^j), \quad (1)$$

where $\hat{\sigma}_{\mu\nu}^j \equiv |\mu\rangle_{jj}\langle\nu|$ are the projection ($\mu = \nu$) or transition ($\mu \neq \nu$) operators for atom j , while $\Delta_{ij} = C_6/r_{ij}^6$ is the strength of the (repulsive, $C_6 > 0$) van der Waals interaction between the Rydberg-excited atoms i and j separated by distance r_{ij} .

Our aim is to prepare the ground state of Hamiltonian (1) in the classical limit of $\Omega \rightarrow 0$. The complete basis consists of states with $n = 0, 1, 2, \dots, N$ Rydberg excitations. On an N -site lattice, n excitations can be arranged in $\binom{N}{n}$ different ways, which is the dimension of the corresponding subspace \mathbb{H}_n of the total Hilbert space $\mathbb{H} = \sum_{n=0}^N \mathbb{H}_n$. In the absence of interactions, $\Delta_{ij} = 0 \forall i, j \in [1, N]$, all the states in each \mathbb{H}_n are degenerate, having the energy $E_n = -n\delta$. Interactions $\Delta_{ij} > 0$ between the atoms (partially) lift this degeneracy, unless $n = 0$ with $E_0 = 0$ for the zero-excitation state $|R_0\rangle \equiv |gg \dots g\rangle$, or $n = 1$ with $E_1 = -\delta$ for all N single-excitation states and their symmetric superposition $|R_1\rangle \equiv \frac{1}{\sqrt{N}} \sum_j |gg \dots r_j \dots g\rangle$. For $n \geq 2$, the lowest energy states $|R_n^{\min}\rangle$ are the states with the largest separation between the Rydberg excitations: $E_2^{\min} = -2\delta + \frac{C_6}{l^6}$, $E_3^{\min} = -3\delta + \frac{C_6}{l^6} + 2\frac{C_6}{(l/2)^6}$, $E_4^{\min} = -3\delta + \frac{C_6}{l^6} + 2\frac{C_6}{(2l/3)^6} + 3\frac{C_6}{(l/3)^6}, \dots$, and more generally

$$E_n^{\min} = -n\delta + \frac{C_6(n-1)^6}{l^6} \sum_{k=1}^{n-1} \frac{k}{(n-k)^6} \simeq -n\delta + \frac{C_6(n-1)^7}{l^6}, \quad (2)$$

where $l = a(N-1)$ is the length of the system, i.e., the distance between the first and last atoms, with a the lattice constant. The energy spectrum $\{E_n\}$ versus detuning δ is schematically shown in Fig. 1. For negative detunings $\delta = \delta_0$, the ground state of the system corresponds to the $n = 0$ excitation state $|R_0\rangle$ with $E_0 = 0$, while for positive $\delta \simeq \delta_n$ the ground state corresponds to the lowest-energy n excitation state $|R_n^{\min}\rangle$, such that $E_n^{\min} < E_{n\pm 1}^{\min}$ which leads to $\delta_n \simeq \frac{C_6 n^7}{2l^6}$.

In the adiabatic preparation protocol [22–26], we start with the state $|R_0\rangle$ and the laser detuning having some negative value $\delta < 0$ which we then slowly increase till reaching some positive final value $\delta \simeq \delta_n$. As we vary the detuning, the energies $E_{0,1,\dots,n}^{\min}$ cross at around $\delta_{0 \rightarrow 1} = 0$, $\delta_{1 \rightarrow 2} = \frac{C_6}{l^6}$, $\delta_{2 \rightarrow 3} \simeq \frac{C_6 2^7}{l^6}$, \dots , $\delta_{(n-1) \rightarrow n} \simeq \frac{C_6((n-1)^7 - (n-2)^7)}{l^6}$ [22]. Of course, with vanishing field amplitude $\Omega \rightarrow 0$, there is no coupling and thereby transitions between the energy levels E_n , and the system initially in state $|R_0\rangle = |gg \dots g\rangle$ will remain in that state irrespective of δ . Hence, as we change the detuning, the field Ω should be non-zero when the energy levels $E_{0,1,\dots,n}^{\min}$ cross, which would lead to avoided crossings and adiabatic following of the ground state of the system. The initial state with zero Rydberg excitations $|R_0\rangle$ is coupled by the field to the symmetric single excitation state $|R_1\rangle$ with the collectively-enhanced rate

$$\Omega_{0 \rightarrow 1} = \sqrt{N}\Omega,$$

which leads to a large level repulsion $\pm\Omega_{0 \rightarrow 1}$ in the vicinity of $\delta_{0 \rightarrow 1}$. Next, state $|R_1\rangle$ is coupled to the lowest-energy double-excitation state $|R_2^{\min}\rangle \equiv |r_1g \dots gr_N\rangle$ with a much smaller rate of

$$\Omega_{1 \rightarrow 2} = \frac{2\Omega}{\sqrt{N}},$$

and the corresponding level repulsion around $\delta_{1 \rightarrow 2}$ is small $\pm\Omega_{1 \rightarrow 2}$. In turn, state $|R_2^{\min}\rangle$ is coupled to the lowest-energy triple-excitation state $|R_3^{\min}\rangle \equiv |r_1g \dots gr_{(N+1)/2}g \dots gr_N\rangle$ (assuming odd N) with the single-atom transition rate

$$\Omega_{2 \rightarrow 3} = \Omega,$$

and the levels are repelled by $\pm\Omega_{2 \rightarrow 3}$ around $\delta_{2 \rightarrow 3}$. The lowest-energy four-excitation state $|R_4^{\min}\rangle \equiv |r_1g \dots gr_{(N+2)/3}g \dots gr_{(2N+1)/3}g \dots gr_N\rangle$ (assuming $N = 6k + 1$ with $k = 1, 2, 3, \dots$) is coupled to the three-excitation state $|R_3^{\min}\rangle$ only via three-photon process, and thus the transition amplitude is small [22],

$$\Omega_{3 \rightarrow 4} \propto \frac{\Omega^3}{[C_6/(l/3)^6]^2}.$$

The successive transitions to higher $n \geq 4$ excitation states involve $(2n-5)$ -photon processes yielding therefore even smaller transition amplitudes $\Omega_{(n-1) \rightarrow n}$.

As we change the laser detuning, our intention [22–24, 26] is that, in the vicinity of $\delta_{(n-1) \rightarrow n}$, the system

adiabatically follows the ground state $|R_{n-1}^{\min}\rangle \rightarrow |R_n^{\min}\rangle$. According to the Landau-Zener formula [27, 28], the probability of non-adiabatic transition $|R_{n-1}^{\min}\rangle \rightarrow |R_n^{\min}\rangle$ is given by $p_{n.a.} \sim \exp(-2\pi|\Omega_{(n-1)\rightarrow n}|^2/\alpha)$, where $\alpha = \frac{\partial}{\partial t}|E_{n-1}^{\min} - E_n^{\min}| = \frac{\partial}{\partial t}\delta$ is determined by the rate of change of detuning δ . Hence, due to the small values of the effective Rabi frequencies $\Omega_{(n-1)\rightarrow n}$ for $n \geq 4$, adiabatic population of states beyond $n = 3$ will be difficult to achieve. We therefore mainly focus on preparing adiabatically the triple-excitation state $|R_3^{\min}\rangle$, but we will briefly consider longer lattices which can accommodate $n = 4$ excitations under otherwise similar conditions. Notice also the bottleneck for the transition $|R_1\rangle \rightarrow |R_2^{\min}\rangle$, due to the smallness of the effective Franck-Condon factor ($f = 2/\sqrt{N}$) of $\Omega_{1\rightarrow 2}$, as compared to $\Omega_{0\rightarrow 1}$ ($f = \sqrt{N}$) and $\Omega_{2\rightarrow 3}$ ($f = 1$). As will be illustrated below, this fact has rather interesting implications for the adiabatic preparation of the target double- and triple-excitation states $|R_2^{\min}\rangle$ and $|R_3^{\min}\rangle$.

We shall consider unitary dynamics of the system, as well as the influence of relaxation processes. These include spontaneous decay of atoms from the Rydberg state $|r\rangle$ to the ground state $|g\rangle$ with rate Γ_r , and dephasing of the atomic transition $|g\rangle \leftrightarrow |r\rangle$ with rate Γ_z due to non-radiative collisions with the background atoms, external and trapping field noise, Doppler broadening, laser linewidth, and decay of the intermediate atomic state $|e\rangle$ to the ground state $|g\rangle$ when $|g\rangle \leftrightarrow |r\rangle$ is a two-photon transition [18, 26]. The corresponding Lindblad generators for the decay and dephasing processes are $\hat{L}_r^j = \sqrt{\Gamma_r}\hat{\sigma}_{gr}^j$ and $\hat{L}_z^j = \sqrt{\Gamma_z}(\hat{\sigma}_{rr}^j - \hat{\sigma}_{gg}^j)$, and the total decay rate of coherence $\langle\hat{\sigma}_{rg}\rangle$ on the transition $|g\rangle \leftrightarrow |r\rangle$ is then $\gamma_{rg} \equiv \frac{1}{2}\Gamma_r + 2\Gamma_z$ [17, 29]. We assume closed systems in which $\hat{\sigma}_{gg}^j + \hat{\sigma}_{rr}^j = \mathbf{1}^j \forall j \in [1, N]$ is preserved throughout evolution.

To simulate the dissipative dynamics of the many-body system, we employ the quantum stochastic (Monte Carlo) wavefunctions [30]. In each quantum trajectory, the state of the system $|\Psi(t)\rangle$ evolves according to the Schrödinger equation $\partial_t |\Psi\rangle = -\frac{i}{\hbar}\tilde{\mathcal{H}}|\Psi\rangle$ with an effective Hamiltonian

$$\tilde{\mathcal{H}} = \mathcal{H} - \frac{i}{2}\hat{L}\hat{L}^\dagger, \quad (3)$$

where

$$\hat{L}^2 \equiv \sum_j (\hat{L}_r^j \hat{L}_r^j + \hat{L}_z^j \hat{L}_z^j) = \sum_j (\Gamma_r \hat{\sigma}_{rr}^j + \Gamma_z \mathbf{1}^j)$$

is the non-Hermitian part which does not preserve the norm of $|\Psi\rangle$ during the evolution. The evolution is interrupted by random quantum jumps $|\Psi\rangle \rightarrow \hat{L}_{r,z}^j |\Psi\rangle$ with probabilities $W_{r,z}^j \equiv \langle\bar{\Psi}|\hat{L}_{r,z}^j \hat{L}_{r,z}^j |\bar{\Psi}\rangle$, where the normalized wavefunction of the system at any time t is given by $|\bar{\Psi}(t)\rangle = |\Psi(t)\rangle/\sqrt{\langle\Psi(t)|\Psi(t)\rangle}$. The expectation value of any observable \hat{O} of the system is then obtained by averaging over many, $M \gg 1$, independently simulated trajectories, $\langle\hat{O}\rangle = \text{Tr}[\hat{\rho}\hat{O}] =$

$\frac{1}{M}\sum_m \langle\bar{\Psi}_m|\hat{O}|\bar{\Psi}_m\rangle$, while the density operator is given by $\hat{\rho}(t) = \frac{1}{M}\sum_m |\bar{\Psi}_m(t)\rangle\langle\bar{\Psi}_m(t)|$.

We define the populations of the lowest-energy n -excitation states as $P_n^{\min} \equiv \langle R_n^{\min}|\hat{\rho}|R_n^{\min}\rangle$. The mean number of Rydberg excitations within an ensemble of N atoms is $\langle n\rangle = \langle\sum_j \hat{\sigma}_{rr}^j\rangle$, while the probabilities $p_n = \langle\hat{\Sigma}_n\rangle$ of n excitations are defined through the corresponding projectors $\hat{\Sigma}_0 \equiv \prod_j \hat{\sigma}_{gg}^j$, $\hat{\Sigma}_1 \equiv \sum_j \hat{\sigma}_{rr}^j \prod_{i \neq j} \hat{\sigma}_{gg}^j$, etc. Obviously $\langle n\rangle = \sum_n n p_n$. To quantify the probability distribution of Rydberg excitations, we use the Mandel Q parameter [31]

$$Q \equiv \frac{\langle n^2\rangle - \langle n\rangle^2}{\langle n\rangle} - 1, \quad (4)$$

where $\langle n^2\rangle = \sum_n n^2 p_n$. A Poissonian distribution $p_n = \langle n\rangle^n e^{-\langle n\rangle}/n!$ leads to $Q = 0$, while $Q < 0$ corresponds to sub-Poissonian distribution, with $Q = -1$ attained for a definite number n of excitations, $p_n = 1$.

In the numerical simulations, we truncate the total Hilbert space to $\max n = 5$ Rydberg excitations and, upon verifying convergence, choose some minimum distance between the excitations, $\min |i - j| \equiv d \geq 1$, which leads to $\dim \mathbb{H}_n^{(d)} = \binom{N-(d-1)(n-1)}{n}$, reducing thereby significantly the computational Hilbert space.

III. RESULTS OF SIMULATIONS

In our simulations, we use system parameters similar to those in recent experiments [18, 26], i.e., we assume ^{87}Rb atoms in a lattice with $a = 532$ nm excited from the ground state $|g\rangle \equiv |5S_{1/2}, F = 2, m_F = -2\rangle$, by a two-photon process via a non-resonant intermediate state $|e\rangle \equiv |5P_{3/2}, F = 3, m_F = -3\rangle$, to the Rydberg state $|r\rangle \equiv |43S_{1/2}, m_J = -1/2\rangle$ with the van der Waals interaction constant $C_6 \simeq 2\pi \times 2.45 \text{ GHz } \mu\text{m}^6$. The time-dependent Rabi frequency $\Omega(t)$ and detuning $\delta(t)$ of the excitation laser(s) are also chosen to have similar values to those in Ref. [26], which were optimized for preparing the $n = 3$ Rydberg excitation ground state in a $N \sim 20$ site lattice. We note that the precise shape of the $\Omega(t)$ pulse of certain duration τ and the corresponding linear variation of $\delta(t)$ are important for the quantitative characterization of the final state of the system, but the general conclusions of our study are qualitatively valid for other similar preparation strategies involving pulsed $\Omega(t)$ with simultaneous monotonic increase of $\delta(t)$ [22–25].

In Fig. 2 we show the dynamics of a representative system of $N = 19$ atoms subject to an appropriate laser pulse (top panel) of duration $\tau = 12 \mu\text{s}$ leading, in the unitary regime of $\Gamma_r = \Gamma_z = 0$, to the final probability $p_3 > 0.99$ of $n = 3$ Rydberg excitations and quite large population $P_3^{\min} \simeq 0.73$ of the target ground state. This preparation time τ is significantly longer than in the experiment [26] with $\tau \simeq 4 \mu\text{s}$, but obtaining the target ground state $|R_3^{\min}\rangle$ with higher probability of

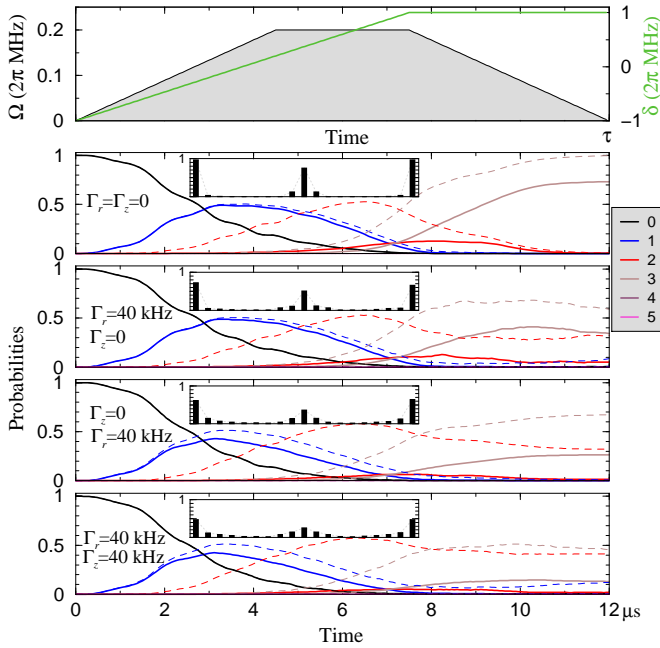


FIG. 2. Dynamics of the system with $N = 19$ atoms initially in the ground state $|R_0\rangle$, subject to the time-dependent field with the Rabi frequency $\Omega(t)$ (left vertical axis) and detuning $\delta(t)$ (right vertical axis) shown in the top panel. The lower panels show the time-dependence of probabilities p_n of n Rydberg excitations (dashed lines) and populations P_n^{\min} of the lowest-energy n -excitation states $|R_n^{\min}\rangle$ (thick solid lines), for $n = 0, 1, \dots, 5$, in the absence or presence of atomic decay Γ_r and dephasing Γ_z . The inset in each panel shows the corresponding spatial structure of the Rydberg excitation probabilities $\langle \hat{\sigma}_{rr}^j \rangle$ of atoms $j = 1, 2, \dots, N$ at the final time τ . The graphs with decay and dephasing were obtained upon averaging over $M = 150 - 200$ independent realizations (Monte-Carlo trajectories) of the numerical experiment.

$P_3^{\min} > 0.9$ would require even slower preparation with $\tau \gtrsim 20 \mu\text{s}$ (see Fig. 3). If we now add realistic decay and/or dephasing of the atoms, the population P_3^{\min} of the target final state would considerably decrease, see Fig. 2. Simultaneously, the spatial distribution of Rydberg excitations, while still retaining order imposed by the open boundary conditions [14, 16, 17], will resemble perfect crystal even less.

In Fig. 3 (top panel), we show the fidelity $F \equiv P_3^{\min}$ of attaining the target crystalline state of $n = 3$ Rydberg excitations in the $N = 19$ site lattice, for unitary ($\Gamma_r = \Gamma_z = 0$) and dissipative ($\Gamma_{r,z} \neq 0$) cases, as a function of the preparation time τ [varying τ means rescaling by the same amount the time-dependence of both $\Omega(t)$ and $\delta(t)$, see Fig. 2 (top panel)]. We observe that, in all cases, the fidelity is rather low, $F \lesssim 0.2$ for $\tau = 4 \mu\text{s}$ [26]. The resulting spatial distribution of Rydberg excitation probabilities $\langle \hat{\sigma}_{rr}^j \rangle$ is also very similar in all cases of Γ_r, Γ_z .

In order to obtain a suitable measure for crystalline order in the finite system, we fit the central peak of

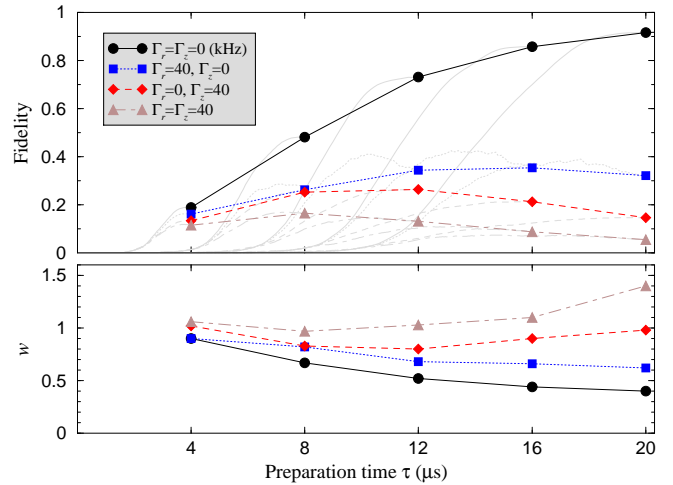


FIG. 3. Final fidelity $F \equiv P_3^{\min}$ (top panel), and corresponding width w (in units of a) of the spatial distribution of $\langle \hat{\sigma}_{rr}^j \rangle$ at the lattice center $j_c = 10$ (bottom panel), versus the preparation time τ , in the $N = 19$ site lattice (as in Fig. 2) for various values of relaxation constants Γ_r, Γ_z (see the legend).

$\langle \hat{\sigma}_{rr}^j \rangle$ in the vicinity of $j_c = (N + 1)/2$ with a Gaussian $\langle \hat{\sigma}_{rr}^j \rangle \simeq A \exp[-(j - j_c)^2/(2w^2)]$ and extract its width w shown in Fig. 3 (bottom panel). For $\tau = 4 \mu\text{s}$ we obtain $w \simeq 1a$ for all cases, which corroborates the above assertion that the final spatial density distribution of Rydberg excitation $\langle \hat{\sigma}_{rr}^j \rangle$ with or without relaxations is nearly indistinguishable. Apparently, when the preparation time τ is too short, the system cannot adiabatically follow the sequence of the lowest-lying states $|R_0\rangle \rightarrow |R_1\rangle \rightarrow |R_2^{\min}\rangle \rightarrow |R_3^{\min}\rangle$ and the final state has a significant admixture of the higher lying states which are still, however, mostly within the $n = 3$ excitation subspace due to the large energy gap with the manifold of higher n states.

Increasing the preparation time τ obviously improves the adiabaticity of the unitary evolution attested by the monotonous increase of the final fidelity F of the target state and the decrease of w , as seen in Fig. 3. But when

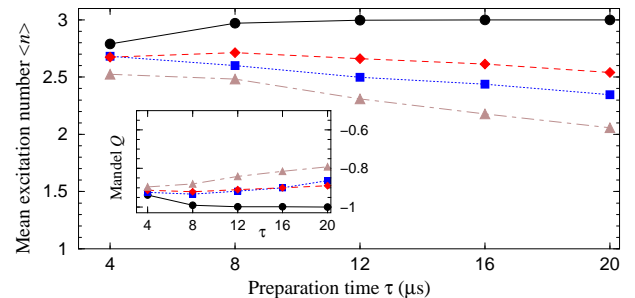


FIG. 4. Mean number of Rydberg excitations $\langle n \rangle$ (main panel) and the corresponding Mandel Q parameter (inset), versus the preparation time τ , for the $N = 19$ site lattice with various Γ_r, Γ_z ; all parameters and correspondence of symbols/lines are the same as in Fig. 3.

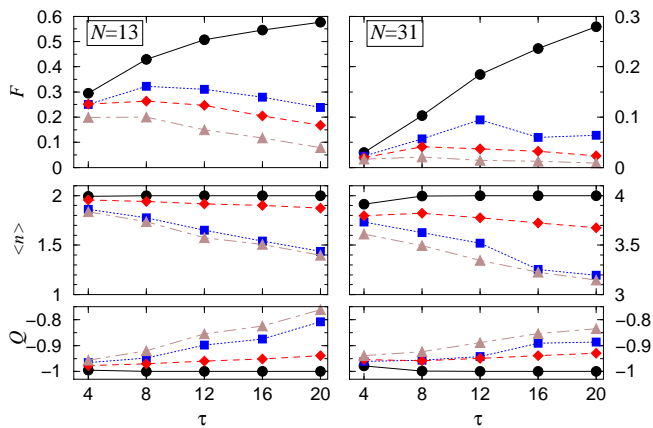


FIG. 5. Fidelities $F \equiv P_2^{\min}$ (top left) and $F \equiv P_4^{\min}$ (top right), mean number of excitations $\langle n \rangle$ (middle) and the corresponding Q parameters (bottom panels), versus the preparation time τ , for the lattice of $N = 13$ (left column) and $N = 31$ (right column) atoms. Notice the difference in the vertical axes scales. All parameters and correspondence of symbols/lines are the same as in Figs. 3 and 4.

we add realistic decay and dephasing, the advantages of slower preparation largely disappear, because the relaxation processes acting for longer time induce more decoherence and deplete the crystalline ground state of the system. Remarkably, the mean number of Rydberg excitations and the corresponding statistics characterized by the highly sub-Poissonian Mandel Q parameter, are considerably less susceptible to relaxations, as shown in Fig. 4. Note that if, for the given parameters of the system, we view the final spatial distribution of Rydberg excitations $\langle \hat{\sigma}_{rr}^j \rangle$ with the corresponding finite resolution w , it would appear nearly indistinguishable from the crystalline state.

As promised above, in Fig. 5 we show the final fidelities, together with the mean excitation numbers and the corresponding Q parameters, for a shorter lattice of $N = 13$ sites that can accommodate $n = 2$ excitations, and for a longer lattice of $N = 31$ sites with up to $n = 4$ excitations, for the same parameters as in the previous figures. The smaller preparation fidelity of the longer $n = 4$ crystal is to be expected, as the system has to adiabatically follow more (avoided) level crossings, the last of which in the vicinity of $\delta_{3 \rightarrow 4}$ has very small level repulsion $\pm \Omega_{3 \rightarrow 4}$. What is more surprising, however, is that, for the same duration τ of the process, the final population of the target double excitation state $|R_2^{\min}\rangle$ in the shorter lattice is smaller than the final population of the target triple-excitation state $|R_3^{\min}\rangle$ in an appropriately longer lattice (cf. Fig. 3). This counter-intuitive behavior can be understood from the following consideration: Due to the small effective coupling $\Omega_{1 \rightarrow 2} = 2\Omega/\sqrt{N}$ between states $|R_1\rangle$ and $|R_2^{\min}\rangle$, and the resulting small level repulsion in the vicinity of $\delta_{1 \rightarrow 2}$, only a fraction of population of state $|R_1\rangle$ is adiabatically converted into the population of the $n = 2$ ground state $|R_2^{\min}\rangle$. On the other

hand, the $n = 3$ crystalline ground state $|R_3^{\min}\rangle$ can be populated not only from state $|R_2^{\min}\rangle$, but also from other higher-energy double-excitation states $|R_2\rangle$ (see Fig. 2). Thus, much of the population remaining in $|R_1\rangle$ after its (avoided) level crossing with $|R_2^{\min}\rangle$ is transferred to the other double-excitation states $|R_2\rangle$, two of which, $|r_1g \dots gr_{(N+1)/2g} \dots gg\rangle$ and $|gg \dots gr_{(N+1)/2g} \dots gr_N\rangle$, can later be converted into $|R_3^{\min}\rangle$. Interestingly, this partial return of population from the higher energy states to the adiabatic ground state of the system leads to its final population which is larger than would follow from a naïve use of the independent, or sequential, level crossing approximation [28].

IV. DISCUSSION AND CONCLUSIONS

To summarize, we have shown that preparing small crystals of merely two to four Rydberg excitations in a lattice gas of several tens of atoms using the adiabatic protocol [22–24] requires exceedingly long times to effect a slow-enough change of detuning of the laser field irradiating the atoms. Then, under typical experimental conditions [18, 26], the relaxation processes affecting the atoms during such long preparation times cause multiple transitions between the diabatic energy levels and deplete the adiabatic crystalline ground state of the system. The resulting mixed final state is then essentially a steady-state of the dissipative system [14, 16] subject to a uniform driving laser with the same final detuning.

In an experiment, the fidelity of preparation of a target crystalline state of n excitations of atoms in a one-dimensional lattice is the probability of simultaneously detecting n Rydberg atoms at equidistant positions, which is obtained from many repetitions of the preparation and site-resolved measurement cycles. In our somewhat idealized treatment, we assumed a perfect lattice of atoms with unity filling of each site, and neglected the motion of Rydberg-excited atoms and their detection errors. Clearly, the initial site-occupation defects of the trapped ground-state atoms, the motion and loss of the untrapped Rydberg-excited atoms, as well as finite detection efficiency will result in further reduction of the measured preparation fidelities of crystalline phases of Rydberg excitations.

While these results may appear discouraging for the prospects of attaining sizable crystals of Rydberg excitations in laser-driven atomic media, our simulations of dissipative dynamics of the system still reveal spatial ordering of Rydberg excitations and highly sub-Poissonian probability distribution of the excitation number, which should not be very sensitive to site-occupation defects. We note that similar and even larger structures can be obtained, or “grown”, perhaps more efficiently if, instead of slowly changing the detuning of the laser uniformly irradiating a chain of atoms initially in the ground state, one sweeps the laser beam with a fixed frequency from the one end of the chain to the other [11].

We hope that our analysis and result are both stimulating and important for the general field of simulating interacting, dissipative many-body systems and imitating their various phases with Rydberg atoms.

ACKNOWLEDGMENTS

This work was supported by the H2020 FET Proactive project RySQ (D.P. and K.M.), the Villum Foundation (K.M.), and the DFG through SFB-TR49 (M.F.). D.P. is grateful to the University of Kaiserslautern for hospitality and to the Alexander von Humboldt Foundation for support during his stay in Germany.

-
- [1] M. Saffman, T.G. Walker, and K. Mølmer, *Rev. Mod. Phys.* **82**, 2313 (2010).
- [2] D. Comparat and P. Pillet, *J. Opt. Soc. Am. B* **27**, A208 (2010).
- [3] M.D. Lukin, M. Fleischhauer, R. Côté, L.M. Duan, D. Jaksch, J.I. Cirac, and P. Zoller, *Phys. Rev. Lett.* **87**, 037901 (2001).
- [4] H. Weimer, R. Löw, T. Pfau, and H.P. Büchler, *Phys. Rev. Lett.* **101**, 250601 (2008).
- [5] H. Weimer and H.P. Büchler, *Phys. Rev. Lett.* **105**, 230403 (2010).
- [6] E. Sela, M. Punk, and M. Garst, *Phys. Rev. B* **84**, 085434 (2011).
- [7] W. Zeller, M. Mayle, T. Bonato, G. Reinelt, and P. Schmelcher, *Phys. Rev. A* **85**, 063603 (2012).
- [8] I. Lesanovsky, *Phys. Rev. Lett.* **106**, 025301 (2011).
- [9] I. Lesanovsky, *Phys. Rev. Lett.* **108**, 105301 (2012).
- [10] T.E. Lee, H. Häffner, and M.C. Cross, *Phys. Rev. A* **84**, 031402(R) (2011).
- [11] M. Höning, D. Muth, D. Petrosyan, and M. Fleischhauer, *Phys. Rev. A* **87**, 023401 (2013).
- [12] M. Höning, W. Abdussalam, M. Fleischhauer and T. Pohl, *Phys. Rev. A* **90**, 021603(R) (2014)
- [13] S. Ji, C. Ates and I. Lesanovsky, *Phys. Rev. Lett.* **107**, 060406 (2011).
- [14] C. Ates and I. Lesanovsky, *Phys. Rev. A* **86**, 013408 (2012); S. Ji, C. Ates, J.P. Garrahan and I. Lesanovsky, *J. Stat. Mech.* P02005 (2013).
- [15] M. Gärttner, K.P. Heeg, T. Gasenzer and J. Evers, *Phys. Rev. A* **86**, 033422 (2012).
- [16] D. Petrosyan, M. Höning, and M. Fleischhauer, *Phys. Rev. A* **87**, 053414 (2013).
- [17] D. Petrosyan, *J. Phys. B* **46**, 141001 (2013); *Phys. Rev. A* **88**, 043431 (2013).
- [18] P. Schauß, M. Cheneau, M. Endres, T. Fukuhara, S. Hild, A. Omran, T. Pohl, C. Gross, S. Kuhr, and I. Bloch, *Nature* **491**, 87 (2012).
- [19] H. Labuhn, D. Barredo, S. Ravets, S. de Léséleuc, T. Macrì, T. Lahaye, A. Browaeys, arXiv:1509.04543.
- [20] J. Otterbach, M. Moos, D. Muth, and M. Fleischhauer, *Phys. Rev. Lett.* **111**, 113001 (2013); M. Moos, M. Höning, R. Unanyan, and M. Fleischhauer, *Phys. Rev. A* **92**, 053846 (2015).
- [21] D. Maxwell, D. J. Szwer, D. Paredes-Barato, H. Busche, J. D. Pritchard, A. Gauguier, K. J. Weatherill, M. P. A. Jones, and C. S. Adams, *Phys. Rev. Lett.* **110**, 103001 (2013).
- [22] T. Pohl, E. Demler, and M. D. Lukin *Phys. Rev. Lett.* **104**, 043002 (2010).
- [23] J. Schachenmayer, I. Lesanovsky, A. Micheli, and A. J. Daley, *New J. Phys.* **12**, 103044 (2010).
- [24] R. M. W. van Bijnen, S. Smit, K. A. H. van Leeuwen, E. J. D. Vredenbregt, and S. J. J. M. F. Kokkelmans, *J. Phys. B* **44**, 184008 (2011).
- [25] B. Vermersch, M. Punk, A. W. Glaetzle, C. Gross, and P. Zoller, *New J. Phys.* **17**, 013008 (2015).
- [26] P. Schauß, J. Zeiher, T. Fukuhara, S. Hild, M. Cheneau, T. Macrì, T. Pohl, I. Bloch, and C. Gross, *Science* **347**, 1455 (2015).
- [27] L.D. Landau, *Phys. Z. Sowjetunion* **2**, 46 (1932); C. Zener, *Proc. R. Soc. A* **137**, 696 (1932); E.C.G. Stückelberg, *Helv. Phys. Acta* **5**, 370 (1932); E. Majorana, *Nuovo Cimento* **9**, 43 (1932).
- [28] S. Brundobler and V. Elser, *J. Phys. A* **26**, 1211 (1993).
- [29] P. Lambropoulos and D. Petrosyan, *Fundamentals of Quantum Optics and Quantum Information*, (Springer, Berlin, 2007).
- [30] J. Dalibard, and Y. Castin, and K. Mølmer *Phys. Rev. Lett.* **68**, 580 (1992); R. Dum, P. Zoller, and H. Ritsch, *Phys. Rev. A* **45**, 4879 (1992); C.W. Gardiner, A.S. Parkins, and P. Zoller *Phys. Rev. A* **46**, 4363 (1992); M.B. Plenio and P.L. Knight, *Rev. Mod. Phys.* **70**, 101 (1998).
- [31] L. Mandel, *Opt. Lett.* **4**, 205 (1979).